Thermodynamic and Mechanical Stabilities of Tantalum Nitride

Chao Jiang,[1,*] Zhijun Lin,[2,†] and Yusheng Zhao[2,‡]

[1]*Structure/Property Relations Group (MST-8), Los Alamos National Laboratory, Los Alamos, New Mexico 87545, USA*
[2]*LANSCE—Lujan Neutron Scattering Center, Los Alamos National Laboratory, Los Alamos, New Mexico 87545, USA*

(Received 1 August 2009; published 28 October 2009)

We perform first-principles density functional calculations on a newly discovered tantalum nitride with an orthorhombic U_2S_3 structure to assess its thermodynamic and mechanical stabilities. Our random search unveils a tetragonal Ta_2N_3 structure that is energetically more favorable than an orthorhombic Ta_2N_3 at zero pressure. We predict that the tetragonal Ta_2N_3 transforms into the orthorhombic phase above a relatively low pressure of 7.7 GPa. Single-crystal elastic constant calculations reveal that orthorhombic Ta_2N_3 is mechanically unstable because of a negative c_{66}. Our calculations suggest that minor oxygen substitution for nitrogen plays an important role in stabilizing the orthorhombic Ta_2N_3 structure.

DOI: 10.1103/PhysRevLett.103.185501 PACS numbers: 62.20.F−, 61.50.Ah

Nitrides synthesized under high-pressure and high-temperature (high *P-T*) conditions represent an important family of materials with enormous potentials for a wide variety of applications. Cubic boron nitride, for example, is the third hardest material after only diamond and BC_2N [1,2]. Searching for nitrides with superior mechanical and chemical properties has been a subject of continuing efforts in the past decade. Several important nitrides have been discovered. The cubic spinel-structured γ-Si_3N_4, synthesized at 15 GPa and 2000 K, is a high-hardness refractory ceramic with Vickers hardness $H_v = 30$–43 GPa and is thermally stable in air up to as high as 1673 K [3,4]. High-pressure syntheses also unveiled a new form of the group-V nitride, P_3N_5, which is quenchable to ambient conditions and represents the first example of fiver-coordinated P in nitridophosphates [5]. Nitrides of the group-IV elements having a cubic Th_3P_4 structure (c-A_3N_4, A = Zr, Hf) were developed [6]. Noble metal (e.g., Pt and Ir) nitrides that display high bulk moduli have also been synthesized [7,8].

Very recently, Zerr *et al.* synthesized a tantalum nitride having an orthorhombic U_2S_3 structure [space group (SG) *Pbnm*] under high *P-T* conditions [9]. Orthorhombic Ta_2N_3 displays a high hardness and peculiar texture, which makes it a highly promising candidate for applications as a hard and fracture-resistant material. In this Letter, first-principles calculations were performed on this newly discovered nitride to examine its stability, crystal and electronic structures, and mechanical properties. A pressure-induced tetragonal-to-orthorhombic phase transformation of Ta_2N_3 is predicted to occur. Furthermore, oxygen-induced stabilization of orthorhombic Ta_2N_3 structure is revealed in this work.

First-principles calculations were performed using the all-electron projector augmented wave method within the generalized gradient approximation of Perdew, Burke, and Ernzerhof [10], as implemented in VASP [11]. In view of the small energy differences between the different candidate structures, a cutoff energy of 500 eV and dense k-point meshes were used to guarantee high numerical accuracy for both total energy and stress calculations. By computing the quantum mechanical forces and stress tensor, all structures were fully relaxed using a conjugate-gradient scheme. The lattice constants for orthorhombic Ta_2N_3 ($a = 8.19$ Å, $b = 8.24$ Å, and $c = 3.00$ Å) obtained by the present calculations are within 1% deviation from the experimental data of Zerr *et al.* ($a = 8.19$ Å, $b = 8.18$ Å, and $c = 2.98$ Å) [9]. The computed internal atomic coordinates of Ta atoms are also in excellent agreement with the experimentally reported values [Table I]. For N atoms, because of their weak scattering power, there are experimental difficulties in accurately determining their positions, as was also pointed out by Zerr *et al.* [9]. This explains the larger differences between first-principles calculated and experimentally measured positional parameters of N atoms.

Using a plasma-enhanced chemical vapor deposition method, Ganin *et al.* [12] synthesized a Ta_2N_3 compound

TABLE I. First-principles predicted internal atomic coordinates of orthorhombic and tetragonal Ta_2N_3. Numbers shown in parentheses are experimental data from Ref. [9].

Phase	Atom	x	y	z
Orthorhombic	Ta1 (4c)	0.313 (0.313)	−0.021 (−0.020)	1/4
	Ta2 (4c)	0.505 (0.505)	0.306 (0.307)	1/4
	N1 (4c)	0.875 (0.875)	0.046 (0.025)	1/4
	N2 (4c)	0.549 (0.585)	0.879 (0.890)	1/4
	N3 (4c)	0.200 (0.201)	0.220 (0.248)	1/4
Tetragonal	Ta1 (2g)	1/2	0	0.756
	N1 (2g)	1/2	0	0.140
	N2 (1c)	1/2	1/2	1/2

 © 2009 The American Physical Society

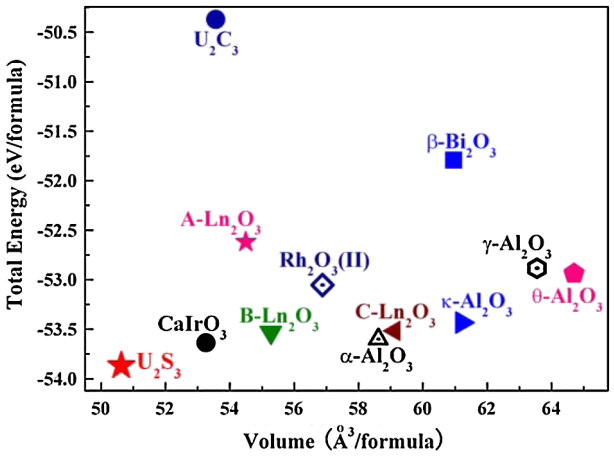

FIG. 1 (color online). First-principles calculated total energies and equilibrium volumes for Ta_2N_3 in various competing crystal structures.

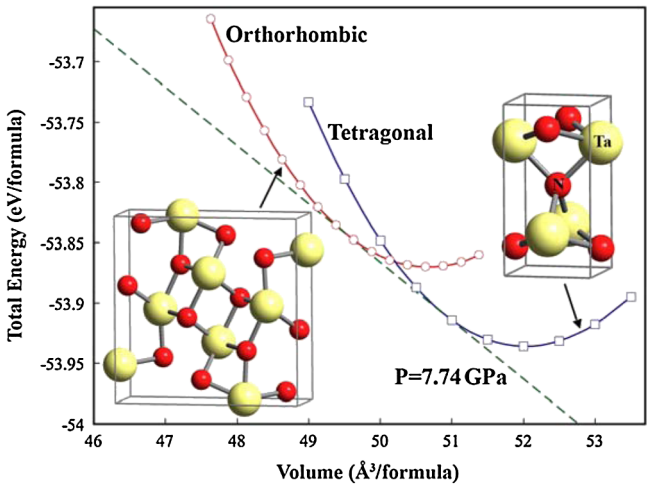

FIG. 2 (color online). Energy-volume (E-V) relationship for Ta_2N_3 in orthorhombic U_2S_3 and tetragonal Rh_3P_2 structures. Their crystal structures are also shown as insets. Large and small spheres represent Ta and N atoms, respectively.

in the bixbyite (C-Ln_2O_3) structure. In an effort to assess the thermodynamic stability of the experimentally observed U_2S_3-type Ta_2N_3 phase, we calculated the total energies of a number of competing crystal structures for Ta_2N_3, including cubic C-Ln_2O_3 (SG $Ia\bar{3}$), hexagonal A-Ln_2O_3 (SG $P\bar{3}m1$), monoclinic B-Ln_2O_3 (SG $C2/m$), trigonal α-Al_2O_3 (SG $R\bar{3}c$), orthorhombic κ-Al_2O_3 (SG $Pna2_1$), monoclinic θ-Al_2O_3 (SG $C2/m$), triclinic γ-Al_2O_3 (SG $P1$), tetragonal β-Bi_2O_3 (SG $P\bar{4}2_1c$), and cubic U_2C_3 (SG $I\bar{4}3d$). The two high-pressure polymorphic structures of Al_2O_3, orthorhombic Rh_2O_3(II) (SG $Pbcn$) and orthorhombic $CaIrO_3$ (SG $Cmcm$) [13], have also been included in our calculations. Among the 12 candidate structures considered, the U_2S_3-type structure is indeed energetically most stable for Ta_2N_3 [Fig. 1]. Furthermore, the U_2S_3-type Ta_2N_3 phase possesses the highest density.

In addition to the "rounding up the usual suspects" approach that is based on the known crystal structures, we performed random structural searches [14,15] in an effort to identify hitherto unsuspected low-energy structures for Ta_2N_3. We generated 30 initial structures containing 5 atoms (1 f.u.) per unit cell and additionally 30 initial structures with 10 atoms (2 f.u.) per unit cell. Here the cell-vector lengths, angles, and atomic positions were all chosen randomly. First-principles calculations were then used to fully relax each structure to a minimum in energy at zero pressure. Surprisingly, our random search unveils that a tetragonal Ta_2N_3 phase (SG $P\bar{4}m2$, $a = 2.99$ Å, $c = 5.82$ Å), although less densely packed, is energetically even more stable than the U_2S_3-type Ta_2N_3. The tetragonal Ta_2N_3 phase is structurally similar to Rh_3P_2 [16]. As is in the U_2S_3-type Ta_2N_3, Ta atoms are also hepta-coordinated in tetragonal Ta_2N_3: six N atoms form a trigonal prism with one prism face capped by the seventh N atom. In Fig. 2, the total energies of Ta_2N_3 in orthorhombic and tetragonal structures are plotted as a function of volume. Using the common tangent construction, we predict that tetragonal Ta_2N_3 will transform into orthorhombic Ta_2N_3 at a relatively low pressure of 7.7 GPa. This may explain why tetragonal Ta_2N_3 was not observed under high-pressure conditions in Zerr's experiment [9].

Figure 3 presents the electronic density of states (DOS) of orthorhombic and tetragonal Ta_2N_3. Both structures are metallic because of the finite DOS at the Fermi level (E_F). The DOS value at E_F of tetragonal Ta_2N_3 is lower than that of orthorhombic Ta_2N_3, which indicates the higher phase stability of the former. In both structures, we observe a

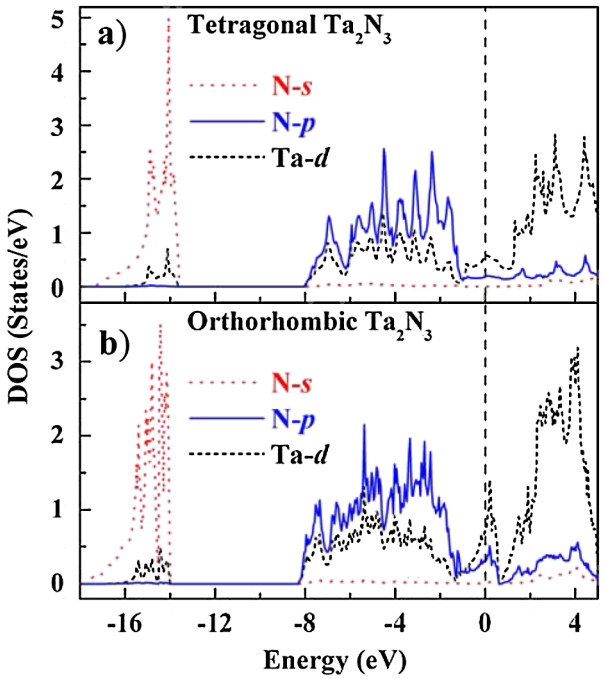

FIG. 3 (color online). Site and angular momentum projected electronic density of states of tetragonal (a) and orthorhombic (b) Ta_2N_3. The vertical dashed line denotes the Fermi level.

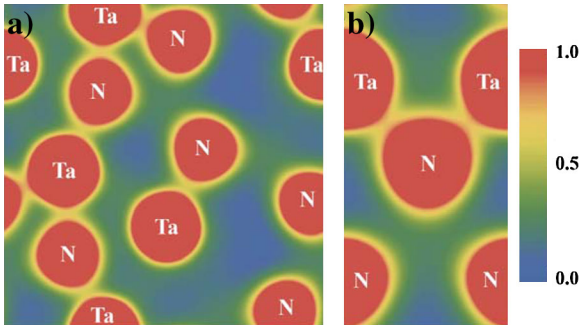

FIG. 4 (color online). Plot of total charge density (in $e/\text{Å}^3$) on the (001) plane of orthorhombic Ta_2N_3 (a) and on the (010) plane of tetragonal Ta_2N_3 (b).

strong hybridization between N $2p$ and Ta $5d$ states, an evidence of covalent bonding between Ta and N atoms. The directionality of covalent Ta-N bonds can also be seen from the charge density distribution plot [Fig. 4]. In contrast to the known structures of platinum dinitrides [17,18], Fig. 4 clearly shows that N atoms do not form N_2 dimers in Ta_2N_3 structures. Indeed, the nearest-neighbor N-N distance in orthorhombic (tetragonal) Ta_2N_3 is 2.43 (2.57) Å, which is much larger than the N-N single bond length (1.45 Å in N_2H_4). Bader charge density analysis [19] further indicates a significant charge transfer from Ta to N atoms, suggesting an ionic contribution to the bonding. The covalent-ionic nature of Ta-N bonding and the absence of covalent N-N bonding in both Ta_2N_3 structures are also confirmed by our electron localization function calculations.

For a structure to be mechanically stable, its strain energy must be positive against any homogeneous elastic deformation [20]. To evaluate the mechanical stability of tetragonal and orthorhombic Ta_2N_3 phases, we calculated their independent single-crystal elastic constants using an efficient strain-stress method [21]. Interestingly, while the elastic constants of tetragonal Ta_2N_3 obey the elastic stability criteria, our calculations indicate that orthorhombic Ta_2N_3 is mechanically unstable due to a negative shear modulus c_{66} [Table II]. As a consequence, orthorhombic Ta_2N_3 undergoes a spontaneous distortion in the x-y plane, resulting in a lower-symmetry monoclinic structure (SG $P2_1/m$) with $\gamma = 91.7°$. In the experimental work, the Ta_2N_3 compound prepared by Zerr *et al.* [9] contains ~3 at.% oxygen. It is thus plausible that oxygen impurity may play a crucial role in stabilizing the orthorhombic Ta_2N_3 structure. To simulate the effects of oxygen, we constructed a 40-atom $1 \times 1 \times 2$ supercell based on the original 20-atom orthorhombic Ta_2N_3 unit cell, in which two of the N atoms were substituted by O. We found that it is energetically most favorable for oxygen atoms to occupy the N3 sites (Table I) in Ta_2N_3. According to our calculations, moving a single oxygen atom from a N3 site to a N1 (N2) site will cost an energy of 0.637 (0.639) eV. Thus, it is assumed that oxygen atoms exclusively occupy the N3 sites. Furthermore, in order to maintain an orthorhombic symmetry of the lattice, there are only two distinct ways in distributing the two oxygen atoms among eight available N3 sites in the supercell, hereinafter referred to as $Ta_{16}N_{22}O_2$-I and $Ta_{16}N_{22}O_2$-II structures [Fig. 5]. Remarkably, the incorporation of a small amount of oxygen significantly increases the shear modulus c_{66} of Ta_2N_3 [Table II], thus making the structure mechanically stable. Electronic DOS calculations further show that minor oxygen substitution for nitrogen reduces the DOS at E_F of orthorhombic Ta_2N_3, which provides another line of evidence for the oxygen-induced stabilization.

In order to evaluate the thermodynamic feasibility of incorporating oxygen into the Ta_2N_3 lattice, the energy change associated with the following oxidation reaction was estimated using first-principles calculations:

$$8Ta_2N_3 + O_2 = Ta_{16}N_{22}O_2 + N_2. \quad (1)$$

Here we obtained the total energies of O_2 and N_2 molecules using a $10 \times 10 \times 10$ Å^3 unit cell. The equilibrium length of the N-N triple bond was calculated to be 1.11 Å, in excellent agreement with an experimentally determined value of 1.09 Å. The predicted O-O double bond length (1.23 Å) also agrees well with the experimental value (1.21 Å). Importantly, the energy change of such a reaction is strongly negative (−6.79 eV for $Ta_{16}N_{22}O_2$-I and −6.50 eV for $Ta_{16}N_{22}O_2$-II), indicating that minor substitution of nitrogen by oxygen in orthorhombic Ta_2N_3 is thermodynamically very favorable. This explains why it is difficult to prevent oxygen uptake during the synthesis of Ta_2N_3 [9]. Finally, we have simulated the x-ray diffraction patterns (not shown for brevity) for $Ta_{16}N_{22}O_2$-I and $Ta_{16}N_{22}O_2$-II, and our results are in good agreement with the experimental data of Zerr *et al.* [9].

From the calculated c_{ij}, the polycrystalline bulk modulus B and shear modulus G can be estimated using the

TABLE II. Single-crystal elastic constants c_{ij} (GPa) of pure and oxygen-bearing Ta_2N_3 from the present first-principles calculations. Polycrystalline bulk modulus B (GPa), shear modulus G (GPa), Young's modulus E (GPa), and Poisson's ratio υ are calculated using the Hill's approximation. EOS fitted bulk moduli B_{EOS} and its pressure derivative B_0' are also shown.

Structure	c_{11}	c_{22}	c_{33}	c_{12}	c_{23}	c_{13}	c_{44}	c_{55}	c_{66}	B	G	E	υ	B_{EOS}	B_0'
Ta_2N_3-Orthorhombic	456	610	639	248	176	203	165	193	−54	327	···	···	···	323	4.45
$Ta_{16}N_{22}O_2$-I	487	531	649	230	166	193	153	188	175	315	173	438	0.269	313	4.59
$Ta_{16}N_{22}O_2$-II	481	581	646	235	170	194	153	176	147	322	167	426	0.279	319	4.37
Ta_2N_3-Tetragonal	684	684	587	147	187	187	152	152	146	333	180	459	0.270	331	4.32

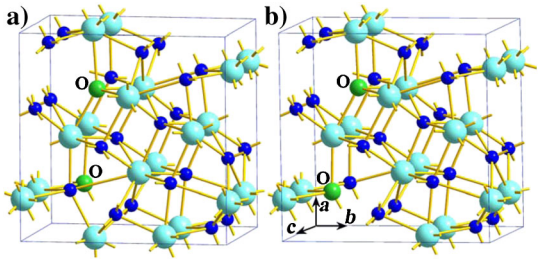

FIG. 5 (color online). Crystal structures of $Ta_{16}N_{22}O_2$-I (a) and $Ta_{16}N_{22}O_2$-II (b). Two oxygen atoms are labeled. The rest of the large and small spheres denote Ta and N atoms, respectively.

Voigt-Reuss-Hill approximation [22]. The bulk modulus can also be directly determined by fitting the calculated total energies at different volumes to an integrated third-order Birch-Murnaghan equation of state (EOS). As shown in Table II, the EOS fitted bulk moduli are in very good agreement with those calculated from the second order elastic constants, which further validates the reliability of the present calculations. Compared to the theoretical elastic properties of the known hard nitrides Zr_3N_4 ($B = 218$ GPa and $G = 129$ GPa) and Hf_3N_4 ($B = 228$ GPa and $G = 138$ GPa) [23], the oxygen-bearing orthorhombic $Ta_{16}N_{22}O_2$ structures possess higher elastic stiffness. According to Teter [24], the polycrystalline shear modulus is a better predictor of hardness than bulk modulus. The average of the shear moduli for $Ta_{16}N_{22}O_2$-I and $Ta_{16}N_{22}O_2$-II is 170 GPa, which corresponds to a theoretical H_v of 27 GPa based on the empirical relationship from Teter ($H_v = 0.1769G - 2.899$ GPa) [24]. This value is in good agreement with that predicted by Zerr *et al.* [9] for a fully dense Ta_2N_3 sample ($H_v = 30$ GPa). Finally, it can be seen from Table II that the tetragonal Ta_2N_3 phase exhibits larger bulk and shear moduli than the oxygen-bearing orthorhombic Ta_2N_3 and is therefore likely to be a hard material as well. Future study on this nitride will be of great interest.

In summary, we carried out first-principles calculations to evaluate the thermodynamic and mechanical stabilities of a newly synthesized orthorhombic Ta_2N_3 phase. Interestingly, using the random search technique, we unveil a tetragonal Ta_2N_3 structure that is more stable than orthorhombic Ta_2N_3 under ambient conditions. The orthorhombic Ta_2N_3, however, becomes the thermodynamically preferred phase at pressures above ~7.7 GPa. Electronic structure calculations reveal that tantalum nitrides in both structures are metallic and their high hardness can be attributed to strong covalent-ionic Ta-N bonds. Our calculations also show that orthorhombic Ta_2N_3 is mechanically unstable and that the substitution of minor oxygen for nitrogen atoms plays a vital role in stabilizing the orthorhombic Ta_2N_3 lattice.

All calculations were performed using the parallel computing facilities at Los Alamos National Laboratory (LANL). This research was supported by LANL, which is operated by Los Alamos National Security, LLC under DOE Contract No. DEAC52-06NA25396.

*chao@lanl.gov
†zlin@lanl.gov
‡yzhao@lanl.gov

[1] V. L. Solozhenko, D. Andrault, G. Fiquet, M. Mezouar, and D. C. Rubie, Appl. Phys. Lett. **78**, 1385 (2001).
[2] Y. Zhao, D. W. He, L. L. Daemen, T. D. Shen, R. B. Schwarz, Y. Zhu, D. L. Bish, J. Huang, J. Zhang, G. Shen, J. Qian, and T. W. Zerda, J. Mater. Res. **17**, 3139 (2002).
[3] A. Zerr, G. Miehe, G. Serghiou, M. Schwarz, E. Kroke, R. Riedel, H. Fuesz, P. Kroll, and R. Boehler, Nature (London) **400**, 340 (1999).
[4] J. Z. Jiang, F. Kragh, D. J. Frost, K. Stahl, H. Lindelov, and J. P. C. Matter, J. Phys. Condens. Matter **13**, L515 (2001).
[5] K. Landskron, H. Huppertz, J. Senker, and W. Schnick, Angew. Chem., Int. Ed. **40**, 2643 (2001).
[6] A. Zerr, G. Miehe, and R. Riedel, Nature Mater. **2**, 185 (2003).
[7] E. Gregoryanz, C. Sanloup, M. Somayazulu, J. Badro, G. Fiquet, H. K. Mao, and R. J. Hemley, Nature Mater. **3**, 294 (2004).
[8] J. C. Corwhurst, A. F. Goncharov, B. Sadigh, C. L. Evans, P. G. Morral, J. L. Ferreira, and A. J. Nelson, Science **311**, 1275 (2006).
[9] A. Zerr, G. Miehe, J. W. Li, D. A. Dzivenko, V. K. Bulatov, H. Höfer, N. Bolfan-Casanova, M. Fialin, G. Brey, T. Watanabe, and M. Yoshimura, Adv. Funct. Mater. **19**, 2282 (2009).
[10] J. P. Perdew, K. Burke, and M. Ernzerhof, Phys. Rev. Lett. **77**, 3865 (1996).
[11] G. Kresse and J. Furthmuller, Phys. Rev. B **54**, 11 169 (1996).
[12] A. Y. Ganin, L. Kienle, and G. V. Vajenine, Eur. J. Inorg. Chem. **2004**, 3233 (2004).
[13] K. Umemoto and R. M. Wentzcovitch, Proc. Natl. Acad. Sci. U.S.A. **105**, 6526 (2008).
[14] C. J. Pickard and R. J. Needs, Phys. Rev. Lett. **97**, 045504 (2006).
[15] Y. Yao, J. S. Tse, and D. D. Klug, Phys. Rev. Lett. **102**, 115503 (2009).
[16] E. H. Ghadraoui, R. Guerin, and M. Sergent, Acta Crystallogr. Sect. C **39**, 1493 (1983).
[17] R. Yu, Q. Zhan, and X. F. Zhang, Appl. Phys. Lett. **88**, 051913 (2006).
[18] A. F. Young, J. A. Montoya, C. Sanloup, M. Lazzeri, E. Gregoryanz, and S. Scandolo, Phys. Rev. B **73**, 153102 (2006).
[19] G. Henkelman, A. Arnaldsson, and H. Jonsson, Comput. Mater. Sci. **36**, 354 (2006).
[20] J. F. Nye, *Physical Properties of Crystals* (Oxford University Press, Oxford, 1985).
[21] C. Jiang, Appl. Phys. Lett. **92**, 041909 (2008).
[22] R. Hill, Proc. Phys. Soc. London **65**, 350 (1952).
[23] M. Mattesini, R. Ahuja, and B. Johansson, Phys. Rev. B **68**, 184108 (2003).
[24] D. M. Teter, MRS Bull. **23**, 22 (1998).